

## Use of poxvirus display to select antibodies specific for complex membrane antigens

Ernest S. Smith, Leslie A. Balch, Maria Scrivens, Shuying Shi, Wei Wang, Caroline D. Harvey, Angelica A. Cornelison, Malgorzata Gil-Moore, Renee A. Kirk, Loretta L. Mueller, Richard L. Hall, Alan P. Howell, Christine A. Reilly, Jessica M. Mayer, Francis G. Murante, Kari A Viggiani, Elaine M. Gersz, Holm Bussler, Madeleine R. Keefe, Elizabeth E. Evans, Mark J. Paris & Maurice Zauderer

**To cite this article:** Ernest S. Smith, Leslie A. Balch, Maria Scrivens, Shuying Shi, Wei Wang, Caroline D. Harvey, Angelica A. Cornelison, Malgorzata Gil-Moore, Renee A. Kirk, Loretta L. Mueller, Richard L. Hall, Alan P. Howell, Christine A. Reilly, Jessica M. Mayer, Francis G. Murante, Kari A Viggiani, Elaine M. Gersz, Holm Bussler, Madeleine R. Keefe, Elizabeth E. Evans, Mark J. Paris & Maurice Zauderer (2023) Use of poxvirus display to select antibodies specific for complex membrane antigens, *mAbs*, 15:1, 2249947, DOI: [10.1080/19420862.2023.2249947](https://doi.org/10.1080/19420862.2023.2249947)

**To link to this article:** <https://doi.org/10.1080/19420862.2023.2249947>



© 2023 Vaccinex, Inc. Published with license by Taylor & Francis Group, LLC.



Published online: 27 Aug 2023.



Submit your article to this journal [↗](#)



Article views: 2847



View related articles [↗](#)



View Crossmark data [↗](#)



Citing articles: 2 View citing articles [↗](#)

REPORT



## Use of poxvirus display to select antibodies specific for complex membrane antigens

Ernest S. Smith, Leslie A. Balch, Maria Scrivens, Shuying Shi, Wei Wang, Caroline D. Harvey, Angelica A. Cornelison, Malgorzata Gil-Moore, Renee A. Kirk, Loretta L. Mueller, Richard L. Hall, Alan P. Howell, Christine A. Reilly, Jessica M. Mayer, Francis G. Murante, Kari A. Viggiani, Elaine M. Gersz, Holm Bussler, Madeleine R. Keefe, Elizabeth E. Evans, Mark J. Paris, and Maurice Zauderer

Research, Vaccinex, Inc, Rochester, NY, USA

### ABSTRACT

Antibody discovery against complex antigens is limited by the availability of a reproducible pure source of concentrated properly folded antigen. We have developed a technology to enable direct incorporation of membrane proteins such as GPCRs and into the membrane of poxvirus. The protein of interest is correctly folded and expressed in the cell-derived viral membrane and does not require any detergents or refolding before downstream use. The poxvirus is selective in which proteins are incorporated into the viral membrane, making the antigen poxvirus an antigenically cleaner target for *in vitro* panning. Antigen-expressing virus can be readily purified at scale and used for antibody selection using any *in vitro* display platform.

### ARTICLE HISTORY

Received 15 February 2023  
Revised 15 August 2023  
Accepted 16 August 2023

### KEYWORDS

Antibody; GPCR; ion channel; membrane; panning; phage; poxvirus

### Introduction

Therapeutic monoclonal antibodies have emerged as an effective treatment modality over the past three decades, with over 100 monoclonal antibodies approved by the US Food and Drug Administration (FDA) for a wide variety of diseases.<sup>1</sup> Antibodies can have therapeutic benefits over small-molecule drugs because of their specificity, the ability to interact with larger areas on the target, long half-life, effector functions such as cell killing, largely extracellular activity, and safety.<sup>2</sup>

The G protein-coupled receptor (GPCR) family has over 800 members.<sup>3,4</sup> All GPCRs are structurally similar membrane proteins, containing an extracellular N-terminus, seven membrane-spanning  $\alpha$ -helices, and an intracellular C-terminus.<sup>5,6</sup> This structure and membrane-associated conformation is required for their proper functioning.<sup>7</sup> GPCRs play a role in many cell-signaling pathways including responses to neurotransmitters, hormones, and chemokines.<sup>3</sup> Approximately one-third of FDA-approved medications target GPCRs, but almost all of these medicines are small molecules.<sup>8</sup> Antibody discovery against GPCRs has been hampered by the challenges associated with purification of the GPCR while maintaining proper structure.<sup>9</sup> Substantial effort has been devoted to different GPCR purification methods including detergents, micelles, virus-like particles (VLPs), and nanodiscs.<sup>10–12</sup> These methods are time consuming, require receptor-specific optimization, and are not always successful at providing properly folded protein.<sup>2,13</sup> In addition, expression levels of GPCRs are often low and over-expression can be toxic to cells, making it difficult to generate stable cell lines for immunization and cell panning.<sup>14</sup> The ability to discover therapeutic antibodies is critically dependent on the availability of properly folded target antigen in sufficient purity and

quantity. Our goal was to develop a broadly effective technology that would enable rapid purification of a consistent source of properly folded transmembrane protein (GPCR and others), with sufficient purity and quantity for antibody discovery, that can be made widely available.

Poxviruses are enveloped DNA viruses whose life cycle occurs exclusively in the cytoplasm of the host cell.<sup>15</sup> Poxvirus produce two infectious forms of virus. The predominant intracellular mature virion (IMV or MV) is wrapped in a membrane derived from the endoplasmic reticulum and stays inside the cell until it is released by cell lysis. Some IMV is transported along microtubules and wrapped with a membrane derived from the trans-Golgi network and then released outside the cell as an extracellular enveloped virus (EEV).<sup>16</sup> The EEV is responsible for dissemination of the virus *in vitro* and likely *in vivo*.

The best-known poxviruses are smallpox and the vaccine strain Vaccinia virus that was used to eradicate smallpox through a global immunization campaign.<sup>17</sup> Because of its ease of use, broad host cell range, and ability to express virtually any protein, Vaccinia virus has been exploited as a recombinant vector for *in vitro* and *in vivo* protein expression for decades. We previously developed methods to produce cDNA libraries in Vaccinia virus for expression optimization of target antigens and for the incorporation of full-length antibodies into the outer membrane of Vaccinia EEV for antibody selection.<sup>18</sup> Our experiments have shown Vaccinia to be a highly effective vector for expression of mammalian proteins both on the cell surface of infected cells and in the EEV membrane itself.

Vaccinia virus is a BSL2 agent that requires additional containment and safety precautions for use.<sup>19</sup> Modified

vaccinia ankar (MVA) is a BSL1 variant of Vaccinia that was derived by passaging Vaccinia virus over 500 times on primary chicken cells.<sup>20</sup> The resulting MVA strain has deleted approximately 15% of the viral genome and is only able to successfully replicate in avian cells and a few selected mammalian cell lines, including baby hamster kidney (BHK) cells.<sup>21</sup> This improved safety profile makes MVA a more amenable vector for use in downstream antibody discovery applications and for screening functional variants.<sup>22</sup> In this report, we describe the development of a technology to direct membrane proteins such as GPCRs into the EEV membrane of MVA and the use of these antigen virions for antibody discovery in vitro.

## Results

Vaccinia and MVA EEV contain four proteins with surface exposure on the outer EEV membrane (A56R, B5R, A33R, A34R) and two proteins that are completely intraviral (F13L, F12L).<sup>16</sup> A56R is a Type I glycoprotein with its N-terminus outside of the virion and a single pass through the EEV membrane.<sup>23</sup> Previously, we demonstrated that full-length immunoglobulins can be efficiently expressed on both the Vaccinia virion and the infected cell surface when the heavy chain is fused at its C-terminus to the N-terminal fragment of the A56R protein and cells are co-infected with vaccinia expressing an immunoglobulin light chain.<sup>18</sup> Unfused immunoglobulin chains did not incorporate efficiently into the viral membrane. We hypothesized that extracellular domains (ECD) of other Type I proteins similarly fused to A56R would also be targeted for EEV membrane expression. To evaluate this, we created viral constructs expressing Sema4D and Her2 ECD fusions with or without the A56R protein (Figure 1a). To test incorporation of antigen into EEV, we performed a pull-down assay (as described in the Methods). Briefly, an antigen-specific antibody is used to capture the virions in liquid suspension,

similar to an immunoprecipitation assay except that viral titer is the readout instead of western blot. The percentage of virions bound is compared to the unbound fraction by plaque assay. As shown in Figure 1b, the tested fusion proteins are efficiently incorporated into the poxvirus, while non-fusion proteins are not. This is consistent with our previous results that fusion with a poxvirus protein facilitates incorporation into the viral EEV membrane. Importantly, both the Her2 and SEMA4D antibodies used in these assays are known to bind to conformational epitopes.<sup>24,25</sup> In order to further support that the tag fusion does not interfere with expression or folding, cells were infected with virus encoding fused or unfused protein and tested by flow cytometry. This assay does not measure incorporation into the virus, it evaluates expression of the protein on the cell surface. The equivalent recognition of fused and non-fused proteins by antibodies that bind to conformational epitopes supports that the fusion does not interfere with expression or folding (Figure 1c). This data supports that the proteins incorporated into the viral membrane are folded and oriented correctly.

Poxvirus can be easily scaled and large amounts of EEV readily harvested and purified by simple centrifugation steps.<sup>19,26,27</sup> The ability to direct properly folded and functionally oriented multi-pass proteins into the outer envelope of poxvirus EEV allows for a consistent source of native antigen for antibody discovery. Because poxvirus is selective in what proteins are incorporated into the virion, poxvirus antigen recombinants express the fusion protein of interest along with only four native viral surface proteins. This makes the antigen-expressing poxvirus a much cleaner reagent than panning on whole cells or other methods like VLPs that have random incorporation of other cellular proteins. To compare protein incorporation, equal protein loads of VLPs and poxvirus were labeled with biotin and evaluated by Western Blot (Figure 1d). Poxvirus samples demonstrated fewer biotinylated proteins than VLPs. Similar results were obtained using both

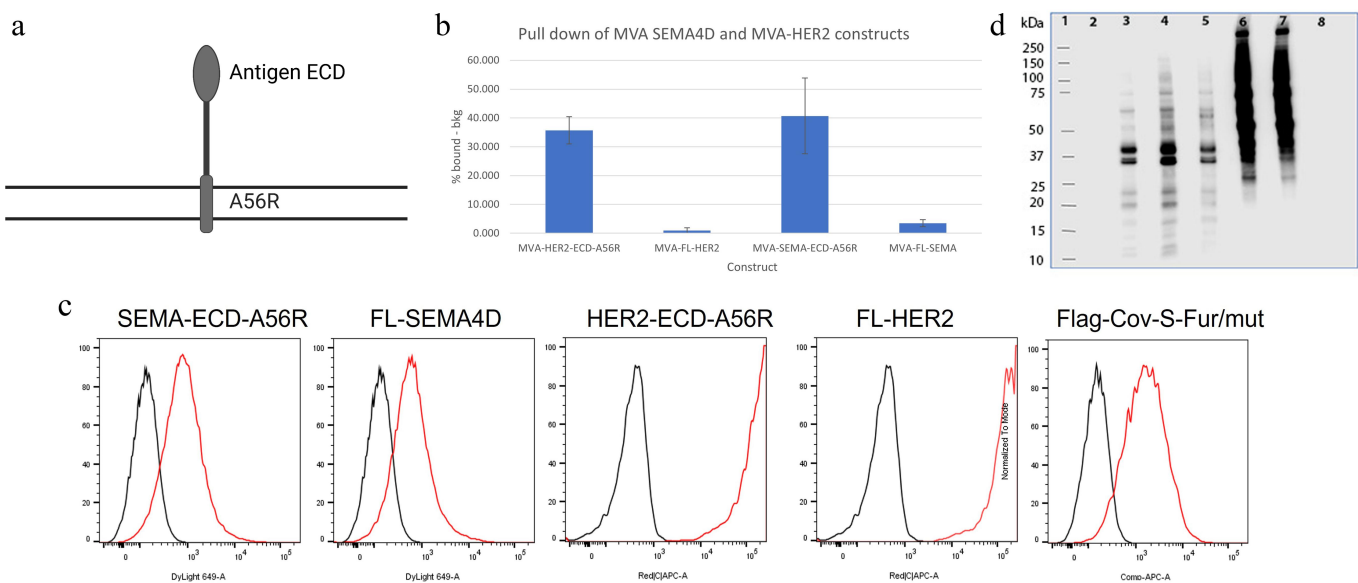


**Figure 1.** (a) Diagram depicting a fusion of antigen (oval) fused to the vaccinia A56 protein. The parallel lines represent the outer membrane of the vaccinia extracellular enveloped virus (EEV). (b) Preferential incorporation of A56-tagged antigen vs untagged antigen. The indicated viral constructs were tested for incorporation of antigen by pull-down assay. (c) Expression of the indicated viral constructs was tested by flow cytometry. (d) Western blot of biotinylated EEV and virus-like particles (VLPs). Equal amounts of protein from the indicated samples were biotinylated and membrane proteins visualized by western blot using streptavidin-HRP detection. Lanes are as follows: 1 Molecular weight standard, 2 CXCR5 virions without biotin, 3 biotin-CXCR4 virions, 4 biotin-CXCR5 virions, 5 biotin-GPR65 virions, 6 biotin-CCR7 VLPs, 7 biotin-Nav1.8 VLPs, and 8 CCR7 VPs without biotin. All samples were loaded with equal protein concentration by BCA assay.

a membrane penetrant biotinylation reagent and a non-penetrant reagent (not shown).

We next wanted to evaluate the use of these virions as a source of antigen for antibody discovery. After first optimizing methods of capture (by ELISA plate or magnetic bead), we used various ECD and GPCR recombinant EEV for in vitro panning with our proprietary phage display library. A number of preliminary experiments were performed to optimize the coating of EEV onto ELISA plates and magnetic beads, and to demonstrate that phage and yeast do not bind nonspecifically to poxvirus (data not shown). We were then able to test the utility of poxvirus expressing heterologous proteins as the antigen source for in vitro panning with phage display libraries.

### Sema4D selection

For our initial selections on antigen-expressing virus, we elected to use Sema4D-ECD-A56R. As shown in Figure 2, we tested selection methods with virus immobilized onto ELISA plate or onto magnetic beads. A phage Fab display library of approximately  $1.5 \times 10^{10}$  unique clones was panned on virus bound to beads or ELISA plates. For panning on

virus antigen, prior to the second, third, and fourth rounds of panning, the antibody library was depleted on control poxvirus to remove anti-virus binding antibodies. After the fourth round of panning, the V genes from the bulk phage were subcloned into a mammalian expression vector for expression as secreted human IgG1, while maintaining the VH and VL pairing that was expressed in each phage. Individual clones were arrayed in 96-well plate format in what we term a mini-library (ML). Each ML was transfected into CHO-S cells in 96-well plates, and secreted antibody was produced over 3 days. The supernatant was cleared of cells and debris by centrifugation and tested for binding to Sema4D positive and negative cells by flow cytometry as well as binding to Sema4D protein by ELISA. Representative histograms for binding by flow cytometry are shown in Figure 3. A total of 1500 clones were screened for binding, and the plasmid DNA from 101 specific clones were sequenced. All unique antibodies were rescreened as described to confirm binding. Over 25 unique antibodies were discovered, with the majority being found only once, suggesting a diverse pool of additional antibodies in the original phage pan. A summary of some

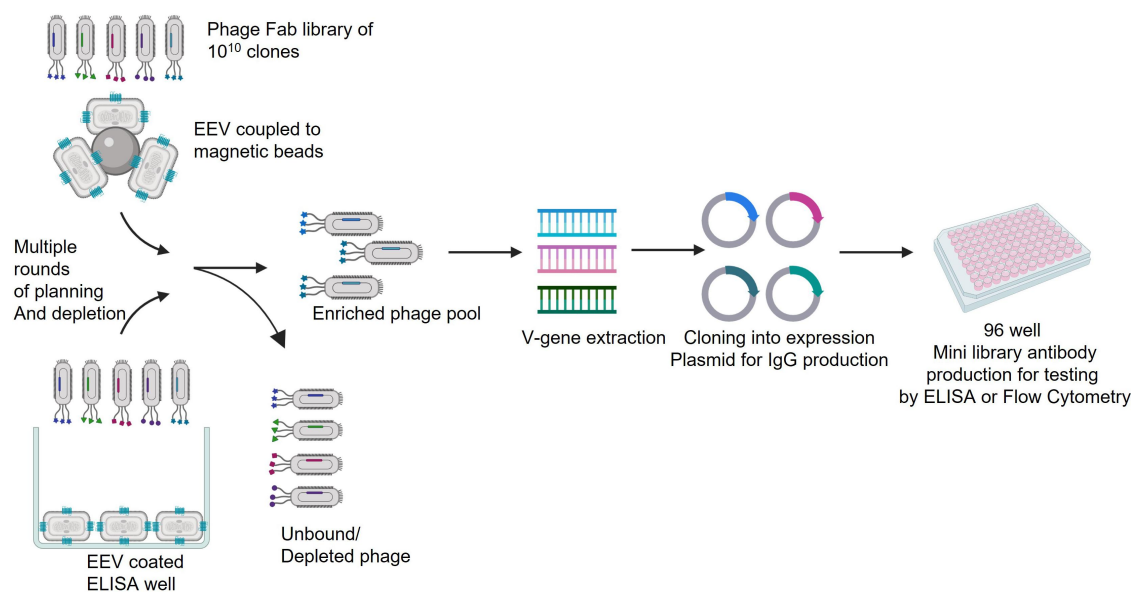


**Figure 2.** Panning scheme. Antigen-expressing virus was either coupled to magnetic beads or ELISA plates. A phage Fab display library containing approximately  $1 \times 10^{10}$  unique clones was added to coupled EEV for 2 hr at room temperature. Following extensive washing, bound phage was expanded following standard procedures. For each subsequent round of selection, the amount of input phage was reduced by  $1/10^{\text{th}}$  and virus-specific binders were reduced by depleting the phage with control virus. After four rounds of selection, the selected V genes were subcloned from phage into a mammalian expression vector for expression as secreted human IgG and selected antibodies tested for antigen binding by flow cytometry.

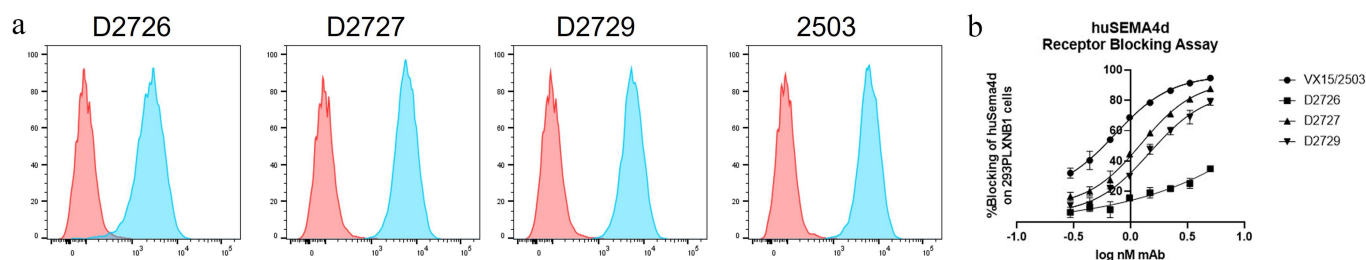


**Figure 3.** (a) Selected antibodies were tested by flow cytometry for binding to Sema4D-positive Jurkat cells (blue) vs Sema4D-negative cells A431 (red). (b) Selected antibodies were tested for the ability to block Sema4D binding to Plexin B1+ cells and compared to VX15/2503 (ref).

**Table 1.** Selection of Sema4D-specific antibodies.

Mab #	Heavy Chain V gene	HCDR3	Light Chain V gene	Frequency	Binding Ratio	ELISA OD	Affinity (nM)
MabD2702	IGHV1-18*01	SSVVGSDWFDY	IGKV1-6*02	5	52	0.734	5
MabD2726	IGHV3-9*01	DGYSDDGLSFDY	IGLV3-1*01	3	29	1.219	50
MabD2727	IGHV3-48*02	DLGGMDV	IGLV3-1*01	1	72	1.553	6
MabD2728	IGHV4-39*07	DQGGLDY	IGLV3-1*01	2	38	1.006	5
MabD2729	IGHV3-48*02	DVAVAGEPLHS	IGLV3-1*01	1	68	1.804	22
MabD2736	IGHV3-74*02	EGPGIRAFDI	IGLV3-1*01	1	61	0.812	40
MabD2737	IGHV1-18*01	EIPGYGVVDV	IGLV3-1*01	1	72	0.783	3
MabE2034	IGHV1-46*03	GDYDWFDP	IGLV1-51*01	1	197	1.0125	2
MabE2036	IGHV3-48*02	DEDAHIHDY	IGLV3-1*01	1	202	1.0325	13
MabE2037	IGHV3-15*05	DFRRGGDN	IGLV3-1*01	1	237	0.658	15

The antibody number and Heavy Chain and Light Chain V gene usage are shown for a subset of Sema4D-specific antibodies. Binding ratio indicates the fold increase in binding of each antibody to Sema4D-positive cells (Jurkat) over binding to Sema4D-negative cells by flow cytometry at 1 µg antibody per 1E6 cells. ELISA OD on recombinant protein at 1 ng/ml of antibody and affinity was measured as described in Materials and Methods.

of the selected antibodies is shown in Table 1. Panning on both plates and beads resulted in similar selected antibodies. Each unique antibody was tested for specificity on a panel of cell lines and by ELISA on various control antigens as well as on a biotinylated cell lysate. Four of these antibodies were purified and tested for the ability to block Sema4D binding to its PlexinB1 receptor.<sup>25</sup> Two of the antibodies blocked similar to the VX15/2503 clinical antibody pepinemb.<sup>25</sup>

Collectively, this data demonstrates that virus expressing antigen can be used to select antibodies that bind to native antigen with good affinity, specificity, and functional activity.

### Her2 selection

For Her2/neu, virus was coated onto an ELISA plate for panning. After four rounds of panning, 500 clones were screened as per the screening methods described above. Ninety-four clones bound specifically to Her2/Neu, from which 16 unique antibodies were identified. A summary of 10 representative antibodies is shown in Table 2. Affinity measurements indicated that the best selected antibodies were in the range of the affinity of chimeric 4D5 (parent antibody of trastuzumab (Herceptin®)).

### SARS-CoV-2 S protein selection

The ease with which recombinants can be made in this system lends itself to rapid production of poxvirus expressing coat

proteins from other viruses such as SARS-CoV-2. The ECD of the S protein of SARS-CoV-2 was expressed as a fusion with A56R and recombinant poxvirus made. Expression analysis indicated that this poxvirus expressed S protein was recognized by specific antibodies by flow cytometry (Figure 1c). The S protein expressing poxvirus was used for in vitro panning on virus coated beads as described above. The top five antibodies with good binding activity and specificity are shown in (Table 3). Antibodies were tested for the ability to block SARS-CoV-2-S protein from binding to ACE2 receptor by ELISA and by flow cytometry. The ranking of antibodies in both these assays agreed. The top antibody was tested in a cell-based blocking assay and demonstrated blocking activity similar to that of Bamlanivimab (Figure 4).

### F13L fusion

The A56R fusion described above is most useful for the ECD of a membrane protein where it can be fused to the extracellular C-terminus of the ECD and provide an anchor in the viral membrane. The C-terminus of a GPCR is intracellular, requiring a different fusion partner for viral incorporation that has an intracellular N-terminus. For this purpose, we used the viral F13L protein, a 42 kDa protein that is involved in the wrapping of the EEV membrane.<sup>28,29</sup> The F13L protein is associated with the inner leaf of the EEV membrane by palmitoylation.<sup>16</sup> The N-terminus of F13L is cytoplasmic, allowing for in-frame fusion with the C-terminus of a GPCR of interest. To create fusions, we removed the stop codon from the GPCR, added a Gly-Ser

**Table 2.** Selection of Her2-specific antibodies.

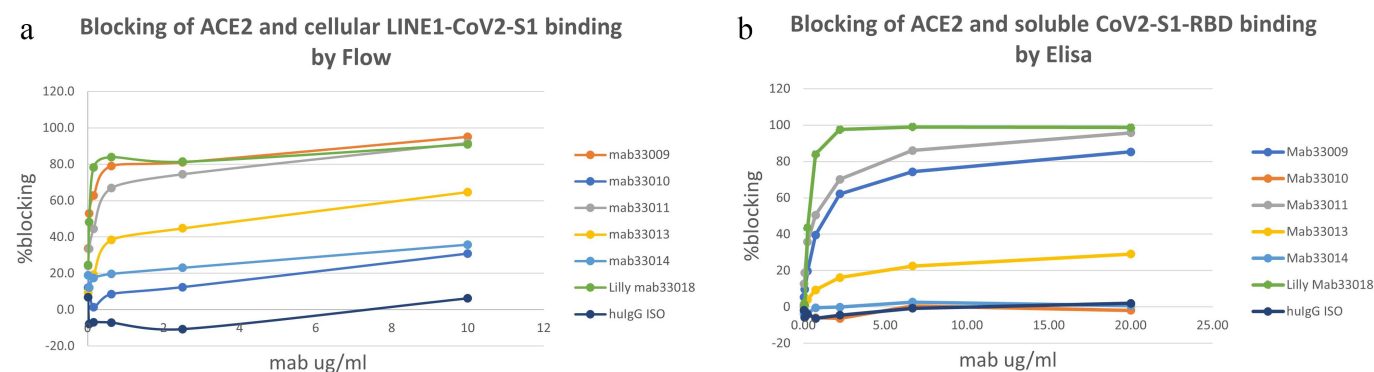
Mab #	Heavy Chain V gene	HCDR3	Light Chain V gene	Frequency	Binding Ratio	ELISA OD	Affinity (nM)
MabC8677	IGHV3-23*01	SRGYYGFDY	IGKV2-30*01	1	676	0.294	13
MabC8678	IGHV3-23*01	NRGYYGFDY	IGKV2-30*01	16	661	0.203	4
MabC8679	IGHV3-11*01	ARGFLGFDY	IGKV2-30*01	1	665	0.245	7
MabC8681	IGHV3-33*05	SDSYSYDSDYFDY	IGLV2-11*02	1	742	0.892	11
MabC8682	IGHV3-11*01	RGGYFPFDY	IGKV2-30*01	1	703	0.284	16
MabC8684	IGHV3-9*01	DGYWGTGD	IGKV2D-28*01	1	265	0.597	4
MabC8685	IGHV3-9*01	RGSRRGGGLDV	IGKV1-5*01	9	373	0.404	5
MabC8686	IGHV1-18*01	DRSYGGGLDV	IGLV2D-28*01	3	741	0.391	35
MabC8690	IGHV3-9*01	NRGYYGFDY	IGKV1D-39*01	1	757	0.531	24
MabC8692	IGHV3-23*01	GRGSYRLFYD	IGKV2D-28*01	2	733	0.581	21
Chimeric 4D5					766	0.530 ± 0.221	1

The antibody number and Heavy Chain and Light Chain V gene usage are shown for a subset of Her2-specific antibodies. Binding ratio indicates the fold increase in binding of each antibody to Her2-positive cells (SKBR3) over binding to Her2-negative cells by flow cytometry at 1 µg antibody per 1E6 cells. ELISA OD on recombinant protein at 1 ng/ml of antibody and affinity was measured as described in Materials and Methods.

**Table 3.** Selection of COV-S-specific antibodies.

Mab#	Heavy Chain V gene	HCDR3	Light Chain V gene	Frequency	Binding ratio	ELISA OD	Cell-based affinity (nM)	RBD affinity (nM)
Mab33009	IGHV3-9*01	PTLPGSSSYGMDV	IGLV2-11*02	1	89	3.0	0.55	2
Mab33010	IGHV1-18*01	DDSRGLDHFDFY	IGLV3-1*01	1	66	3.1	1.72	6.7
Mab33011	IGHV3-23*01	GISNFRDVFVGV	IGLV1-36*01	2	94	3.2	1.05	3.8
Mab33013	IGHV3-9*01	DRLGEWEILGGYLDY	IGLV10-54*01	4	88	2.9	0.67	1.9
Mab33014	IGHV3-15*05	GLPGSGEQWHDDVFDI	IGLV3-25*03	2	97	3.2	0.68	0.3
Bamlanivimab								0.5

The antibody number and Heavy Chain and Light Chain V gene usage are shown for a subset of COV-S-specific antibodies. Binding ratio indicates the fold increase in binding of each antibody to Line 1 cells stably expressing COV-S-RBD over Line 1 vector alone cells by flow cytometry at 1 µg antibody per 1E6 cells. ELISA OD on recombinant protein at 1 ng/ml of antibody and affinity was measured as described in Materials and Methods.

**Figure 4.** Selected antibodies were tested for the ability to block Cov-S protein binding to Ace2 by flow cytometry (a) and ELISA (b).

linker, and then fused in-frame with the N-terminus of the F13L protein. These proteins are efficiently incorporated into poxvirus EEV membrane (Figure 5b) and expressed on the cell surface (Figure 5c). A similar fusion strategy was used for CD20, which also has an intracellular C-terminus, illustrating that this fusion strategy can be effective for other transmembrane proteins besides GPCRs.

The anti-CD20 mouse antibody 2B8 (parental antibody of Rituximab) was used in the pull-down assay and is known to recognize a conformational epitope on the second extracellular loop of CD20.<sup>30,31</sup> To expand upon these results, virus expressing CD20 was coated onto ELISA plates and reactivity with Rituximab and Ofatumumab was tested (Figure 5d). Ofatumumab is known to bind a conformational epitope that is created from both extracellular loops of CD20 and does not overlap with the Rituximab epitope. The strong specific binding of both of these antibodies to the CD20 displayed on the virions confirms that the CD20 is properly folded and presented in the viral membrane. As shown in Figure 5e-f, additional ELISA testing of CXCR4 virions using the mouse monoclonal 12G5 and CCR5 virions using the mouse monoclonal 2D7 (both conformational epitope-specific antibodies for their respective antigens) demonstrated good recognition of the antigen displayed on the virions and supports proper folding and presentation for antibody selection.<sup>31,32</sup>

CD39 is a multi-pass membrane protein that converts ATP into AMP and is a target for antibody therapy for cancer.<sup>33</sup> We constructed poxvirus expressing CD39 and tested the enzymatic activity of the virus. As shown in Figure 5g, the CD39 virus was able to convert ATP into

AMP, demonstrating proper folding and function of the protein expressed on the poxvirus.

#### CXCR4 selection

CXCR4 is a rhodopsin-like GPCR that is widely expressed and controls cell movements in response to its ligand CXCL12.<sup>34,35</sup> Full-length CXCR4 was expressed with a Gly-Ser linker and enhanced green fluorescent protein (eGFP) fluorescent tag in frame with the F13L protein to facilitate incorporation into the EEV virion membrane. A recombinant poxvirus was generated, and four rounds of phage panning were performed on CXCR4 poxvirus coupled to beads as outlined in Figure 2. After ML screening, analysis of 1000 clones resulted in 15 specific clones, from which 12 unique antibodies were identified. Panning on CXCR4 VLPs was unsuccessful, demonstrating the value of tagging the antigen into the virus. The top eight antibodies with binding activity and specificity are shown in Table 4. Six of these antibodies were found only once, suggesting additional unique binders were present in the phage pan. Two of these antibodies were able to block the binding of CXCL12-induced cell migration as effectively as hybridoma-derived antibodies (Figure 6).

#### FZD4 and FZD7 selection

FZD4 and FZD7 are GPCRs that participate in the WNT signaling pathway.<sup>36</sup> Full-length FZD4 and FZD7 were expressed with a Gly-Ser linker in frame with the F13L protein. A recombinant poxvirus was generated, and four rounds of phage panning were performed. For FZD4, panning was performed on virus coated onto an ELISA plate, while FZD7

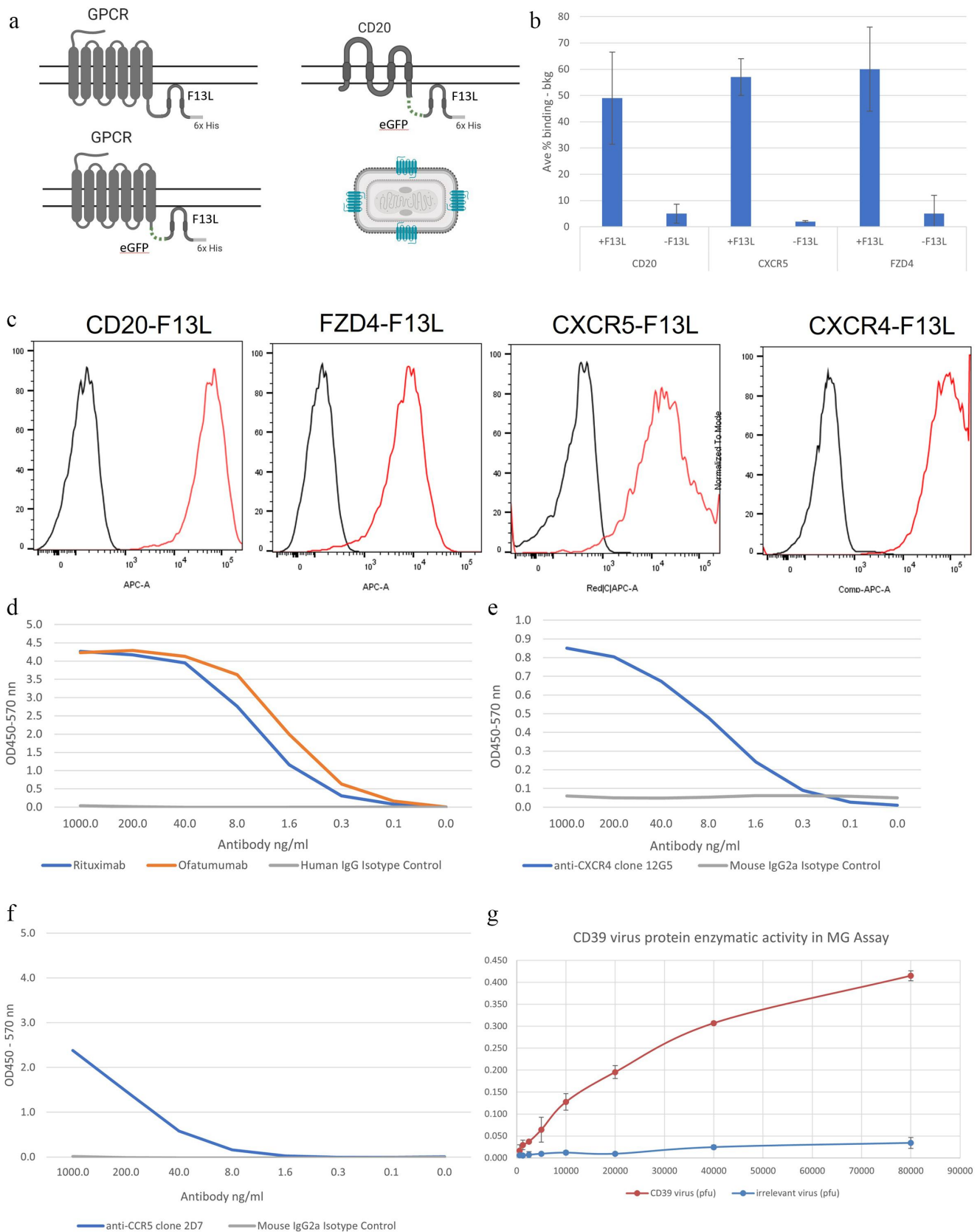


**Figure 5.** (a) Diagram depicting a fusion of antigen fused to the vaccinia F13L protein. The parallel lines represent the outer membrane of the vaccinia extracellular enveloped virus (EEV). (b) Preferential incorporation of F13L-tagged antigen vs untagged antigen. The indicated viral constructs were tested for incorporation of antigen by pull-down assay. (c) Expression of the indicated viral constructs was tested by flow cytometry. Cells were infected with the indicated viral constructs, and after an overnight infection, the cells were harvested and tested for expression of the target antigen by flow cytometry. (d) Antigen expressing or control virus was coated onto ELISA plates at  $5 \times 10^6$  pfu/well and then tested for recognition by specific antibodies by ELISA (d) CD20, (e) CXCR4, and (f) CCR5. (g) The ability of CD39 expressed by poxvirus vs control poxvirus to convert ATP to AMP was tested in a malachite green assay as described in the methods.

**Table 4.** Selection of CXCR4-specific antibodies.

Mab#	Heavy Chain V gene	HCDR3	Light Chain V gene	Frequency	Binding ratio
MabE22328	IGHV3-30*18	GGWLDD	IGLV3-1*01	1	138
MabE22329	IGHV1-18*01	GGN	IGKV2-24*01	2	142
MabE22332	IGHV1-46*03	GRGLAHRGMDV	IGKV1-9*01	1	28
MabE22333	IGHV3-33*05	EKGRKIDY	IGKV2-30*02	1	244
MabE22334	IGHV1-46*03	RYCSRVSCLNGMDV	IGKV1-16*01	4	44
MabE22335	IGHV1-46*03	RPYRGSGLPLS	IGKV1-17*01	2	160
MabE22337	IGHV3-33*05	GLLRYSSWSRSGYGGYGGMDV	IGKV1-6*02	1	55
MabE22338	mIGHV1-69*02	DGGKNFDY	IGKV1-6*02	1	43

The antibody number and Heavy Chain and Light Chain V gene usage are shown for a subset of CXCR4-specific antibodies. Binding ratio indicates the fold increase in binding of each antibody to CXCR4-positive cells (Jurkat) over binding to CXCR4-negative cells by flow cytometry at 1  $\mu$ g antibody per 1E6 cells.

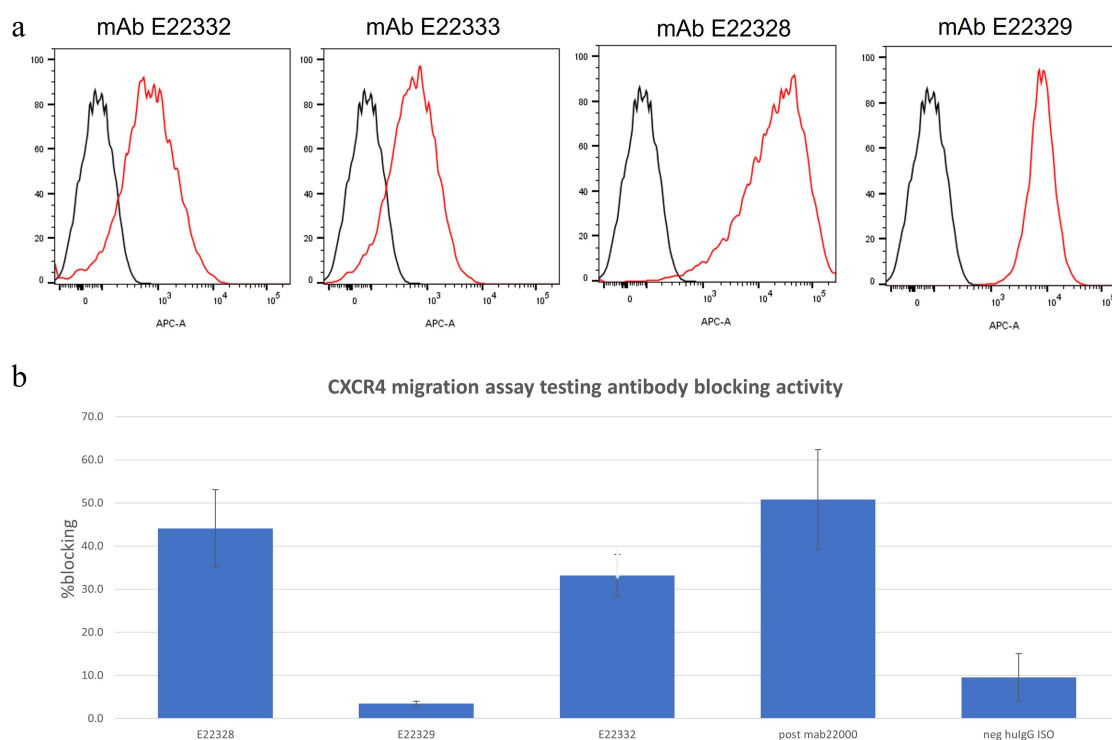


**Figure 6.** (a) Selected antibodies were tested by flow cytometry for binding to CXCR4-positive cells (blue) vs CXCR4-negative cells (red). (b) Selected antibodies were tested for the ability to block CXCR4-induced migration of Jurkat cells.

panning was performed on virus coupled to beads as outlined in Figure 3. Analysis of 500 clones for FZD4 yielded 55 specific clones, resulting in the identification of 17 unique antibodies. For FZD7, screening 400 clones resulted in 46 specific

antibodies which collapsed into 10 unique sequences. A summary of the data is shown in Tables 5 and 6. Antibodies were tested for specificity on FZD4, FZD7, FZD2, and FZD1. Interesting patterns of reactivity were observed for

**Table 5.** Selection of FZD4-specific antibodies.

Mab #	Heavy Chain V gene	HCDR3	Light Chain V gene	Frequency	Binding Ratio on FZD4	Binding Ratio on FZD1	Binding Ratio on FZD2	Binding Ratio on FZD7
MabC6757	IGHV3-33*05	DLLPAMALAGTGALGG	IGKV3-11*01	5	151	1	1	1
MabC6760	IGHV3-33*05	DRLPAMALAGTGALGG	IGKV3-11*01	18	168	1	1	1
MabC6755	IGHV3-33*05	DMLPAMALAGTGALGG	IGKV3-11*01	14	146	1	1	1
MabC6754	IGHV1-46*03	PVIGTNAFDL	IGKV1D-12*02	1	169	1	1	1
MabC6758	IGHV3-33*05	PVIGTNAFDL	IGKV1D-12*02	2	190	1	1	1
MabC6762	IGHV3-23*01	PTIGANAFDI	IGKV3-20*01	1	146	1	1	1
MabC6753	IGHV3-33*05	PVVGAGAFDY	IGKV3-20*01	9	178	1	1	1
MabC6759	IGHV3-33*05	PVVGAGAFDY	IGKV1D-39*01	1	145	1	1	1
MabC6763	IGHV1-46*03	SHVWFRGYFEK	IGLV1-44*01	1	148	1	1	1

The antibody number and Heavy Chain and Light Chain V gene usage are shown for a subset of FZD4-specific antibodies. Binding ratio indicates the fold increase in binding of each antibody to FZD-positive cells over binding to FZD-negative cells by flow cytometry at 1  $\mu$ g antibody per 1E6 cells.

**Table 6.** Selection of FZD7-specific antibodies.

Mab#	VH family	HCDR3	VL/VK family	Frequency	Binding Ratio FZD7	Binding Ratio FZD2	Binding Ratio FZD1
Mab30009	IGHV3-21*02	DPFFGAVDY	IGKV1-6*02	1	215	4	1
Mab30004	IGHV3-21*02	DPYYGAIDY	IGKV1-6*02	1	49	4	2
Mab30007	IGHV3-9*01	DSPVWPPRGYFDS	VK1-09 (L8)	1	48	7	11
Mab30010	IGHV4-39*07	DRFLAPTGLHYFDP	IGKV1-6*02	1	168	51	2
Mab30000	IGHV1-46*03	GPSSRQYGDGFGVMDV	IGLV1-49*01	1	73	6	33
Mab30002	IGHV4-39*07	DRHGTYLDY	IGKV1-6*02	1	86	8	58
Mab30027	IGHV3-33*05	DGFEYSNSGGAYYGLDV	IGKV1-6*02	17	54	23	51
Mab30016	IGHV4-39*07	AAVGVDNWFDP	IGKV1-6*02	3	167	54	160
Mab30021	IGHV4-39*07	DDPSSDGLDY	IGKV1-6*02	1	265	62	201
Mab30022	IGHV6-1*02	DGLSRDHDFWNYGMDV	IGKV1-6*02	1	65	27	48

The antibody number and Heavy Chain and Light Chain V gene usage are shown for a subset of FZD4-specific antibodies. Binding ratio indicates the fold increase in binding of each antibody to FZD-positive cells over binding to FZD-negative cells by flow cytometry at 1  $\mu$ g antibody per 1E6 cells.

**Table 7.** Affinity-improved antibodies.

mAb	Light	Binding Ratio	LCDR1	LCDR2	LCDR3	Affinity (nM)
MabE2132	L2801	104	SGHKLGDLYAY	QDDKRPS	QTWDSNTAV	20
MabE2134	L2799	103	SGETLGDYYIY	RDNRRPS	QAWDSNIAV	8
MabE2141	L2794	103	SGDRLGEYTY	QDGKRPS	QAWDSGTAV	44
MabE2131	L2802	102	SGDKLGDKYAY	QDRKRPS	QTWDSIAV	69
MabE2140	L2795	98	SGDRLGEYTY	QDGKRPS	QAWDSGTAV	53
MabE2138	L2797	98	SGDKLGDLYTY	QDTKRPS	QAWDSSTAV	48
MabE2130	L2793	94	SGDRLGEYTY	QDGKRPS	QAWDSGTAV	52
MabE2137	L2798	91	SGDKLGDLYTY	QDTKRPS	QAWDSSTAV	100
MabD2726	L2525	78	SGDKLGDLYTY	QDTKRPS	QAWDSSTAV	879

The antibody and Light Chain numbers for affinity-improved variants of MabD2726. All antibodies use the same heavy chain = H2456A. Table shows binding ratio and changes in CDRs for the improved light chains. Some antibodies only had changes in the framework regions.

the FZD7-specific antibodies, with some antibodies binding to all three proteins, some binding to FZD7 and FZD1 but not FZD2, and a few being specific to just FZD7. For FZD4, no binding to other FZDs was observed. Panning on untagged FZD4 virus, or FZD4 VLPs was unsuccessful, demonstrating the value of tagging the antigen into the virus.

### Affinity improvement

In order to demonstrate that antigen poxvirus can be used for affinity improvement of antibodies, the VH from MabD2726 that is specific for Sema4D was cloned into a new phage vector with a collection of 200 million diverse light chains. Bead panning followed by competition with unbound Sema4D EEV was performed on Sema4D (see Materials and Methods). After three rounds of affinity improvement screening, clones were tested. As shown in Table 7, several affinity-improved antibodies were selected that used the same germline light chain but had improved affinity. As shown in Figure 7, this improvement in affinity translated into improvement in functional activity.

### Discussion

We describe here a novel technology using a fusion protein strategy to express virtually any membrane protein in the membrane of poxvirus and demonstrate the use of the virus expressing antigen for antibody discovery in vitro. This technology has several advantages over purification strategies using whole cells or VLPs. The fusion protein is properly folded and in the correct, uniform orientation for the activity of the membrane receptor. For antibody discovery, no

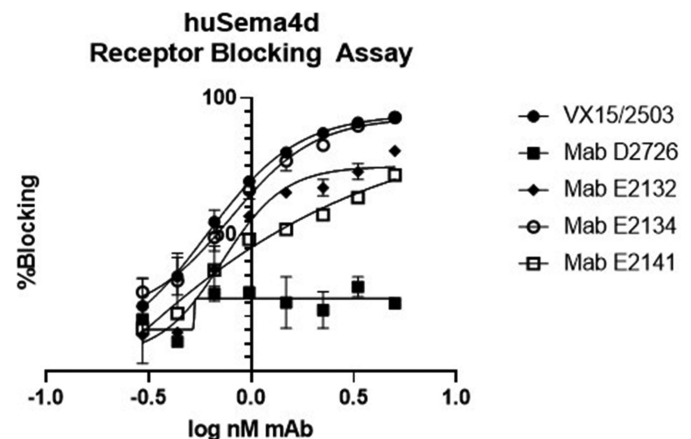


**Figure 7.** Affinity-improved antibodies were tested for the ability to block Sema4D binding to Plexin B1+ cells and compared to VX15/2503 (ref) and parental antibody D2726.

detergents, purification, or refolding is necessary. The virus is simply harvested from the cell culture supernatant by standard centrifugation techniques and can be coated onto magnetic beads or ELISA plates for panning. Poxviruses are selective in which proteins are allowed to be efficiently incorporated into the viral membrane. MVA expressing a recombinant membrane fusion protein will express the antigen of interest along with the standard four known viral surface proteins, A56R, B5R, A33R, A34R. These viral proteins are the same and consistently expressed by all virions produced by any strain of poxvirus. These antigen virions are thus much cleaner and more consistent than whole cells or VLPs, which incorporate any protein in a lipid raft. The consistency of the viral proteins makes depletion of antibodies to the four native viral

membrane proteins straightforward. Antibody discovery coupling viral antigen expression with phage display is a very rapid way to select antibodies. It takes approximately 2 months to generate the virus-expressing antigen, and phage display with these antigen viruses uses similar protocols and timelines as would be used for simple purified proteins. Finally, these antigen virus particles can also be used for affinity improvement of antibodies specific for known membrane proteins.

This technology has been used for a variety of different proteins, including SARS-CoV-2 Spike protein, Her2, CD20, and a number of GPCRs. Antibody selection was successful against all of these types of target molecules. We have not seen a difference in the quality of antibodies selected when panning is done on antigen-expressing virus coated onto ELISA plates or onto beads. Both methods seem equally effective. We have also demonstrated with partners that these antigen-expressing viruses can be used with yeast display. In addition, we have used the antigen virus for in vivo immunization coupled to in vitro panning. This application will be reported separately.

## Materials and methods

### Reagents

All cell lines, including QT35 and BHK-21, were purchased from ATCC. Accutase™ (Sigma-Aldrich) was used for cell detachment, and Dynabeads™ (ThermoFisher) were used for pull-down assays. Antibodies against CD20 were generated in-house to use as controls: 2B8 (Mouse anti-CD20), Rituximab (Human anti-CD20), and Ofatumumab (Human anti-CD20). Additionally, Trastuzumab (Human anti-HER2), Pepinemab (Human anti-SEMA4D), Bamlanivimab (Human anti-SARS-CoV-2 Spike protein), and mAbC6073 (internally discovered Human anti-FZD4) were purified in-house for use as controls. Mouse anti-CXCR5 (clone #51505) was purchased from R&D Systems; mouse anti-CXCR4 (clone #12G5) was purchased from Biologend; and mouse anti-CCR5 (clone #2D7) was purchased from BD Biosciences. Mouse Isotype controls were purchased from Biologend (mouse IgG1,K cat# 401402 Biologend; mouse IgG2a,K cat #401508 Biologend), and Human IgG Isotype control was purchased from Southern Biotech (human IgG1, K cat# 0151-01 Southern Biotech). Secondary detection antibodies were purchased from Invitrogen, Southern Biotech or Biologend Biotin-Goat anti Hu Fc Southern Biotech 2048-08 0.5 mg/mL, Streptavidin-APC Southern Biotech cat#7105-11 M, Biotin-Goat anti-Mouse Fc Biologend cat # 405303.

### Transfer plasmid generation

To generate transfer plasmids for each gene of interest, we first generated a transfer plasmid backbone with multiple cloning sites connecting three cloning cassettes separated by linkers allowing for routine modular cloning. In this way, we were able to create fusion proteins with and without an N-terminal tag such as Flag, Vaccinia protein tag (A56R or F13L), or other tracking tag such as GFP. Synthetic genes for Vaccinia WR A56R (GenBank accession # LT966077), Vaccinia WR F13L (Genbank accession # LT966077), or the indicated target

antigens were synthesized (TWIST or Genewiz) or PCR amplified and cloned into the transfer plasmid backbone using standard molecular biology methods.

### MVA construct generation

MVA was generated by trimolecular recombination<sup>23</sup> in BHK cells using fowlpox virus as helper virus. Following recombination, individual MVA virion plaques were picked and DNA extracted via Qiagen Blood Extraction kit. Recombinants were identified by PCR using vector and target-specific primers. Positive clones were expanded by growth on BHK and titrating on QT35 cells.

### Flow on infected cells

To verify protein expression, QT35 cells grown in a 6-well plate were infected with the MVA construct of interest and an MVA-Null control at a multiplicity of infection (MOI) of 1 virion per cell. The virus was allowed to infect overnight at 37°C, 7% CO<sub>2</sub>. The next morning, the cells were harvested using Accutase, pelleted, and washed with FACS Buffer (1× phosphate-buffered saline (PBS), 1% bovine serum albumin (BSA), and 2 mM EDTA). The cells were then stained using commercially available antibodies against the antigen and isotype controls using standard flow cytometry methods.

### Pull-down and titer of EEV virions expressing antigen

For each sample, 5 µg of antibody was coupled to 25 µl of Protein G Dynabeads™ (ThermoFisher) using the manufacturers recommended protocol. Small-scale EEV supernatant was generated by infecting QT35 in 6-well plates as above at an MOI of 1 and allowed to infect for 2 days. The EEV in the supernatant was collected and spun at 930 × g for 10 min to pellet any cell debris. One milliliter of EEV sup was incubated with 25 µl of antibody-coupled beads and rotated at room temperature for an hour to facilitate antibody capture of the antigen-expressing virus. Positive and negative control combinations were included where possible. The beads were then washed five times. The unbound virus in the washes was saved and pooled and the bound and unbound fractions tittered. The negative control bound percentage was subtracted from this value to give the specific antigen bound percentage.

### CD39 enzyme assay

CD39 MVA EEV protein enzymatic activity was assessed in Malachite Green Assay. The conversion of ATP to AMP by CD39 protein releases free phosphate into the reaction buffer. Malachite Green reacts with free phosphate and is measured as absorbance at 620 nm. This assay is performed in 96-well half-area white clear-bottom plate (Costar 3884). Malachite Green is from ENZO Life Sciences BML-AK 111-0250. ATP is from Thermo Scientific R044. ATP solutions were made in 'TM' assay buffer (25 mM Tris-HCl and 5 mM MgCl<sub>2</sub> plus 0.5% BSA). High absorbance signal equals high CD39 activity.

To perform the experiment, briefly, 5  $\mu$ l of 10X titrated MVA virus (CD39 or control) was added to each well of 96-well half-area white clear-bottom plate, and 40  $\mu$ l of 1.25X ATP solution (final at 100  $\mu$ M) was added to all wells. The plate was sealed incubated at room temperature with shake (40 rpm) for 180 min. The reaction was stopped with 60  $\mu$ l Malachite Green, and the plate was shaken at room temperature for 20 min and absorbance read at 620 nm.

### Large-scale EEV generation

BHK-21 cells are documented to produce EEV virions and were chosen for large scale MVA production.<sup>26,27</sup> BHK-21 cells were seeded onto Corning® Cellstack™ 2-stack culture chambers and allowed to reach confluence. MVA IMV virions for each construct were pre-treated with trypsin and incubated at 37°C for 30 min before dilution in BHK complete media. The diluted virions were added to the Cellstack™ chambers in a minimal volume to cover the monolayers (50 ml) at an MOI = 1. Virus was allowed to infect at 37°C, 7% CO<sub>2</sub> for 1–2 hr before additional BHK complete medium was added (150 ml) and placed back at 37°C, 7% CO<sub>2</sub> for 2 days to produce EEV virions. Culture supernatant containing the EEV was then harvested and spun at 930  $\times$  g rpm for 10 min to pellet any cell debris. The clarified supernatant was then centrifuged at 28,000  $\times$  g for 1 hr to pellet EEV virions. Supernatant was aspirated, and the virus pellet was resuspended in 1 $\times$  PBS, pH 7.4. Pelleted virus was tested in a pull-down assay to verify antigen incorporation by diluting 1:100 in QT35 complete media and then following the procedure as outlined previously. MVA EEV virions were aliquoted and quick frozen before long-term storage at –80°C.

### Phage library construction

cDNA was prepared from Human Bone Marrow total RNA (Clontech636591, Lot #1002008) using standard protocols. RT primers were specific to the constant domain of human heavy Mu and light Kappa and Lambda genes. Heavy chain and light chain (kappa and lambda) variable regions were amplified and cloned separately using V and J primers.<sup>37</sup> Restriction sites were incorporated into the primers for cloning. In addition to fully naïve light chains prepared from human bone marrow cDNA, the library includes a defined set of 21 synthetic germline lights (14 VK and 7 VL). PCR products were subcloned and used to make a phagemid vector expressing Fab fused to phage P3 using standard methods. Total library diversity is ~1.5E10 clones.

### Phage panning

Phage display selection was done following standard methods with some modifications for panning on virus.<sup>38</sup> To select antibodies through phage panning, EEV was coupled either to MyOne Tosylactivated Dynabeads (Invitrogen, 6550) or to Nunc Maxisorp plates (ThermoFisher, 44-2404-21). For bead panning, EEV was coupled to beads by combining 3E8 pfu EEV with 50  $\mu$ l of beads in a final volume of 1 mL PBS, and rotated at 37°C overnight. For plate panning, 100  $\mu$ l of 1E8 pfu/

ml was added to each of 10 ELISA wells and the virus allowed to coat at room temperature overnight. For both beads and plate panning, unbound EEV was removed by washing, and beads/plates were blocked for 2 hr at 37°C with PBS + 10% FBS/1% BSA. For the initial round of selection, a phage Fab display library containing approximately 1E10 unique clones was added to the coupled EEV for 2 hr at room temperature. Following extensive washing, phage bound to beads was added directly to TG1 cells for overnight expansion. Plate-bound phage was washed, eluted with 0.2 M glycine, pH 2.2 + 1 mg/mL BSA, neutralized with 1 M Tris-HCl, pH 9.1 and then added to TG1 cells for overnight expansion. Following the centrifugation of the overnight TG1 cultures, enriched phage was PEG precipitated from supernatant, concentrated by centrifugation, and resuspended in PBS for subsequent rounds of panning. For each additional round of panning, the amount of input phage was decreased by a factor of 10 and depleted for multiple rounds on a control EEV in order to remove anti-virus binding antibodies. Coupling EEV for depletion was done in an identical manner as for selection. Following four rounds of enrichment, the V genes from the phage pool were subcloned into a mammalian expression vector while maintaining the VH and VL pairing that was in each phage

For affinity improvement, input phage library came from selected heavy chains paired with approximately 2E7 novel and unique light chains. Virus coupling was done by adding 3E8 pfu EEV to 50  $\mu$ l MyOne Tosylactivated Dynabeads for the initial round of panning, and then decreasing the amount of both beads and EEV 10-fold from one round to the next. Following each round of selection and bead washing, weakly bound phage was competed off with 3E8 pfu Sema4D-expressing EEV in solution. Phage remaining bound to EEV-coated beads was then extensively washed and expanded as previously described.

### Preparing mini-library from phage pans

Bacterial pellet containing phagemid was obtained from the pan and plasmid DNA was extracted (Qiagen HiSpeed Maxiprep kit, 12662). Expression cassette containing the linked heavy and light chains (variable light-constant light-RBS element-variable heavy) was sub-cloned as a pool into mammalian expression dual gene vector pEFDGV3. The library was plated on four standard 150 mm LB AGAR plates containing 50 mg/mL Kanamycin (LB-Kan50) and incubated overnight at 37°C. Control vector only plate is included. Approximately 5000 colonies were harvested from the plates (10 ml LB/Glycerol per plate was applied to each plate, and colonies are gently lifted from the agar surface using a sterile cell scraper) and plasmid DNA was extracted (QIAprep Spin Miniprep, 27104). This pool was subsequently digested with Sall/BssHI to remove the RBS element and replace it with an IRES element for mammalian co-expression. Ninety-four colonies were picked into 96-well deep-well growth plate containing 1.2 mL/well LB/Kan50 and grown for 22 hr at 37°C. A spot plate was arrayed to allow for future propagation of each individual clone. Plasmid DNA was isolated in this format using the Qiagen turbo 96 kit (27191).

### Mini-library transfection

CHO cells were seeded in 96-well flat-bottom plates at 50,000 cells/well in 10% DMEM and incubated overnight at 37°C, 7% CO<sub>2</sub>. Plasmid clones were transfected at one clone per well using Lipofectamine 2000 (Invitrogen, 11668019) and following the manufacturer's recommendations. Transfection was incubated for 3 days at 37°C, 7% CO<sub>2</sub>, at which point, the plates were centrifuged and the resulting supernatant was transferred to a fresh plate for testing.

### Mini-library screening

Native or stable cell lines expressing the antigen of interest and a negative control were harvested using Accutase (if adherent) and pelleted. Cell pellets were resuspended in FACS Buffer at 4E10<sup>6</sup> cells/ml, and 25 µl was dispensed to each well of a 96-well V-bottom plate (Greiner). Twenty-five microliters of CHO mini-library supernatant was added to each well on both the positive and negative cell lines. Antibody binding was determined by flow cytometry using standard procedures.

### Antibody purification

For large-scale transfection in suspension, CHO cells were seeded at a density of 3E6 cells/mL in a 50:50 mix of FreeStyle F17 Expression media (Gibco, A1383501) and PowerCHO-2 CD (Lonza, BELN12-771Q) and the cells transfected using PEI Max (Polysciences, Inc., 24765). Following approximately 24 hr of 37°C incubation, transfection was shifted to 31°C, 7% CO<sub>2</sub> orbiting at 100 rpm for an additional 5 days. The cells were removed through centrifugation, and the resulting supernatant was filter sterilized for purification.

Antibodies were purified from the supernatant using Mab Capture protein A resin (Thermo, 4374730). Antibody was concentrated to the desired concentration using Amicon Ultra-15 30K filters (Millipore, UFC903024) and then passed through a Mustang E filter (Pall, MSTG25E3) to remove endotoxin. Finally, the purified antibody was passed through a 0.2 µm filter (Pall, 4602) to sterile-filter.

### Sema4D flow blocking assay

To measure the ability of selected antibodies to block the binding of SEMA4D to its receptor PLXNB1, a flow cytometry-based blocking assay was run as described.<sup>27</sup>

### Blocking of SARS-CoV-2 and ACE2 receptor binding

Anti-SARS-CoV-2 antibody functional activity was assessed in a SARS-CoV-2 and ACE2 receptor-binding assay by both ELISA and flow cytometry. For the ELISA-based assay, SARS-CoV-2 RBD protein (Acrobiosystems, SPD-C5255) was coated at 1 µg/mL in PBS on 96-well Nunc flat-bottom Immuno plates and left at room temperature overnight. After three washes, the plates were blocked in a buffer containing PBS + 1% BSA + 0.05% Tween for 1 hr. After three washes, biotinylated human ACE2 (Acrobiosystems, AC2-H82F9) was added at 20 ng/ml in the presence and absence of titrated anti-SARS-CoV-2 antibodies

and left at room temperature for 1–2 hr. After five washes, detection secondary streptavidin HRP (Biosource, SNN4004) was added to the plates for 30–60 min. After five washes, TMB substrate was added for 15 min, followed by stopping with 2 N sulfuric acid. Plates were read at 450–570 nM.

For the flow-based assay, SARS-CoV2-RBD stably transfected Line 1 cells were stained with 100 ng/ml of biotinylated human ACE2 in the presence and absence of titrated anti-SARS-CoV-2 antibodies in FACS buffer for 1 hr on ice. After washing, the cells were stained with APC Streptavidin secondary (Biolegend, 405207) for 30 min on ice. The cells were washed and fixed with 0.5% paraformaldehyde plus propidium iodide staining for live cells and analyzed on BD FACS Canto II. FlowJo flow cytometry software was used for analysis, and APC GMFI was used to calculate percent blocking.

Percentage of blocking was calculated with the following formula:

$$\% \text{ blocking} = 100 \times (1 - (\text{GMFI in the presence of mAb} / \text{GMFI in the absence of mAb}))$$

### CXCR4 migration assay

Anti-CXCR4 antibody functional activity was assessed by measuring the inhibition of Jurkat cell migration induced by SDF-1α. Briefly, 5 × 10<sup>5</sup> Jurkat cells were incubated with and without anti-CXCR4 antibodies (10 µg/ml) in 100 µl of chemotaxis buffer (0.5% BSA+RPMI 1640) at 37°C for 60 min. Later, 100 µl of cell suspension (in triplicates) was transferred to the upper well of Corning Costar Transwell plates where the lower chamber contained 600 µl of 50 ng/ml of human SDF-1α (Sino Biological, 13511-HNCE). Wells without any human SDF-1α were included to measure the spontaneous migration. After 4-hr incubation at 37°C in a 7% CO<sub>2</sub> incubator, the inserts containing non-migrating cells were removed, and 60 µl of Alamar Blue was added to the lower chambers containing migrating cells. Plates were then placed in 37°C 7% CO<sub>2</sub> incubator overnight and then read for Fluor at 530/590 on a BIOTEK Synergy HT plate reader. Percentage of inhibition was calculated with the following formula:

$$\% \text{ of inhibition} = 100 \times (1 - (\text{average cell number with antibody} / \text{average cell number without antibody}))$$

### Abbreviations

BSL: Biosafety level; ECD: Extracellular domain, EEV: Extracellular Enveloped Virus, eGFP: Enhanced Green Fluorescent Protein; GPCR: G protein Coupled Receptor; IMV: Intracellular Mature Virus; MVA: Modified Vaccinia Ankara; Sema4D: Semaphorin 4D; VLP: Virus-Like Particle.

### Acknowledgments

Images in figures were created with Biorender.com

### Disclosure statement

All authors have stock or stock options in Vaccinex, Inc.

## Funding

This work was supported by Vaccinex, Inc.

## References

- Mullard A. FDA approves 100th monoclonal antibody product. *Nat Rev Drug Discov.* 2021;20(7):491–95. doi:10.1038/d41573-021-00079-7.
- Hutchings CJ, Koglin M, Marshall FH. Therapeutic antibodies directed at G protein-coupled receptors. *MAbs.* 2010;2:594–606. doi:10.4161/mabs.2.6.13420.
- Foord SM, Bonner TI, Neubig RR, Rosser EM, Pin JP, Davenport AP, Spedding M, Harmar AJ. International Union of Pharmacology. XLVI. G protein-coupled receptor list. *Pharmacol Rev.* 2005;57:279–88. doi:10.1124/pr.57.2.5. PMID: 15914470.
- Hauser AS, Attwood MM, Rask-Andersen M, Schiöth HB, Gloriam DE. Trends in GPCR drug discovery: new agents, targets and indications. *Nat Rev Drug Discov.* 2017;16:829–42. doi:10.1038/nrd.2017.178.
- Fredriksson R, Lagerström MC, Lundin LG, Schiöth HB. The G-protein-coupled receptors in the human genome form five main families. Phylogenetic analysis, paralogon groups, and fingerprints. *Mol Pharmacol.* 2003;63:1256–72. doi:10.1124/mol.63.6.1256. PMID: 12761335.
- Katritch V, Cherezov V, Stevens RC. Structure-function of the G protein-coupled receptor Superfamily. *Annu Rev Pharmacol Toxicol.* 2013;53(1):531–56. doi:10.1146/annurev-pharmtox-032112-135923. PMID: 23140243.
- Lagerström MC, Schiöth HB. Structural diversity of G protein-coupled receptors and significance for drug discovery. *Nat Rev Drug Discov.* 2008;7:339–57. doi:10.1038/nrd2518. PMID: 18382464.
- Congreve M, de Graaf C, Swain NA, Tate CG. Impact of GPCR Structures on Drug discovery. *Cell.* 2020;181:81–91. doi:10.1016/j.cell.2020.03.003. PMID: 32243800.
- Carter PJ, Lazar GA. Next generation antibody drugs: pursuit of the ‘high-hanging fruit’. *Nat Rev Drug Discov.* 2018;17(3):197–223. doi:10.1038/nrd.2017.227. PMID: 29192287.
- Lundstrom K, Wagner R, Reinhart C, Desmyter A, Cherouati N, Magnin T, Zeder-Lutz G, Courtot M, Prual C, André N, et al. Structural genomics on membrane proteins: comparison of more than 100 GPCRs in 3 expression systems. *J Struct Funct Genomics.* 2006;7(2):77–91. doi:10.1007/s10969-006-9011-2. PMID: 17120110.
- Jo M, Jung ST. Engineering therapeutic antibodies targeting G-protein-coupled receptors. *Experimental & Molecular Medicine.* 2016;48(2):e207. doi:10.1038/emm.2015.105. PMID: 26846450.
- Wiseman DN, Otchere A, Patel JH, Uddin R, Pollock NL, Routledge SJ, Rothnie AJ, Slack C, Poyner DR, Bill RM, et al. Expression and purification of recombinant G protein-coupled receptors: A review. *Protein Expr Purif.* 2020;167:105524. doi:10.1016/j.pep.2019.105524. PMID: 31678667.
- Sarkar CA, Dodevski I, Kenig M, Dudli S, Mohr A, Hermans E, Plückthun A. Directed evolution of a G protein-coupled receptor for expression, stability, and binding selectivity. *Proc Natl Acad Sci U S A.* 2008;105:14808–13. doi:10.1073/pnas.0803103105. PMID: 18812512.
- Dunham JH, Hall RA. Enhancement of the surface expression of G protein-coupled receptors. *Trends Biotechnol.* 2009;27:541–45. doi:10.1016/j.tibtech.2009.06.005. PMID: 19679364.
- Moss B. Membrane fusion during poxvirus entry. *Semin Cell Dev Biol.* 2016;60:89–96. doi:10.1016/j.semcdb.2016.07.015. PMID: 27423915.
- Smith GL, Vanderplasschen A, Law M. The formation and function of extracellular enveloped vaccinia virus. *J Gen Virol.* 2002;83(12):2915–31. doi:10.1099/0022-1317-83-12-2915. PMID: 12466468.
- Moss B. Vaccinia virus: a tool for research and vaccine development. *Sci.* 1991;252(5013):1662–67. doi:10.1126/science.2047875. PMID: 2047875.
- Smith ES, Zauderer M. Antibody library display on a mammalian virus vector: combining the advantages of both phage and yeast display into one technology. *Curr Drug Discov Technol.* 2014;11(1):48–55. doi:10.2174/157016381101140124163634. PMID: 24090134.
- Vaccinia Virus and Poxvirology. vaccinia virus and poxvirology. Vol. 890, 2nd ed. New Jersey: Humana Totowa; 2012.
- Carroll MW, Moss B. Host range and cytopathogenicity of the highly attenuated MVA strain of vaccinia virus: propagation and generation of recombinant viruses in a nonhuman mammalian cell line. *Virology.* 1997;238(2):198–211. doi:10.1006/viro.1997.8845. PMID: 9400593.
- Antoine G, Scheiflinger F, Dorner F, Falkner FG. The complete genomic sequence of the modified vaccinia Ankara strain: comparison with other orthopoxviruses. *Virology.* 1998;244(2):365–96. doi:10.1006/viro.1998.9123. PMID: 9601507.
- Verheust CGM, Pauwels K, Breyer D. Biosafety aspects of modified vaccinia virus Ankara (MVA)-based vectors used for gene therapy or vaccination. *Vaccine.* 2012;30(16):2623–32. doi:10.1016/j.vaccine.2012.02.016.
- DeHaven BC, Gupta K, Isaacs SN. The vaccinia virus A56 protein: a multifunctional transmembrane glycoprotein that anchors two secreted viral proteins. *J Gen Virol.* 2011;92:1971–80. doi:10.1099/vir.0.030460-0. PMID: 21715594.
- Okines AF, Cunningham D. Trastuzumab: a novel standard option for patients with HER-2-positive advanced gastric or gastro-oesophageal junction cancer. *Therap Adv Gastroenterol.* 2012;5(5):301–18. doi:10.1177/1756283x12450246. PMID: 22973416.
- Fisher TL, Reilly CA, Winter LA, Pandina T, Jonason A, Scrivens M, Balch L, Bussler H, Torno S, Seils J, et al. Generation and preclinical characterization of an antibody specific for SEMA4D. *MAbs.* 2016;8(1):150–62. doi:10.1080/19420862.2015.1102813. PMID: 26431358.
- Spehner D, Drillien R, Proamer F, Houssais-Pêcheur C, Zanta MA, Geist M, Dott K, Balloul JM. Enveloped virus is the major virus form produced during productive infection with the modified vaccinia virus Ankara strain. *Virology.* 2000;273:9–15. doi:10.1006/viro.2000.0411.
- Drexler IHK, Wahren B, Erfle V, Sutter G. Highly attenuated modified vaccinia virus Ankara replicates in baby hamster kidney cells, a potential host for virus propagation, but not in various human transformed and primary cells. *Journal of General Virology.* 1998;79(2):347–52. doi:10.1099/0022-1317-79-2-347.
- Schmutz CWR. Release of extracellular particles by recombinant vaccinia virus over-expressing the major envelope protein p37K. *Gen Virol.* 1995;76(12):2963–68. doi:10.1099/0022-1317-76-12-2963.
- Honeychurch KMYG, Jordan R, Hruby DE. The vaccinia virus F13L YPPL motif is required for efficient release of extracellular enveloped virus. *J Virol.* 2007;81(13):7310–15. doi:10.1128/JVI.00034-07.
- Reff ME, Carner K, Chambers KS, Chinn PC, Leonard JE, Raab R, Newman RA, Hanna N, Anderson DR. Depletion of B cells in vivo by a chimeric mouse human monoclonal antibody to CD20. *Blood.* 1994;83(2):435–45. doi:10.1182/blood.V83.2.435.435.
- Klein C, Lammens A, Schäfer W, Georges G, Schwaiger M, Mössner E, Hopfner KP, Umaña P, Niederfellner G. Epitope interactions of monoclonal antibodies targeting CD20 and their relationship to functional properties. *MAbs.* 2013;5(1):22–33. doi:10.4161/mabs.22771. PMID: 23211638.
- Ray-Saha S, Huber T, Sakmar TP. Antibody epitopes on G protein-coupled receptors mapped with genetically encoded photoactivatable cross-linkers. *Biochemistry.* 2014;53(8):1302–10. doi:10.1021/bi401289p.
- Spatola BN, Lerner AG, Wong C, Dela Cruz T, Welch M, Fung W, Kovalenko M, Losenkova K, Yegutkin GG, Beers C, et al. Fully human anti-CD39 antibody potently inhibits ATPase activity in cancer cells via uncompetitive allosteric mechanism. *MAbs.* 2020;12(1):1838036. doi:10.1080/19420862.2020.1838036. PMID: 33146056.

34. Duquenne C, Psomas C, Gimenez S, Guigues A, Carles M-J, Barbuat C, Lavigne J-P, Sotto A, Reynes J, Guglielmi P, et al. The two human CXCR4 isoforms display different HIV receptor activities: Consequences for the emergence of X4 strains. *J Immunol.* 2014;193:4188–94. doi:10.4049/jimmunol.1303298.
35. Roland J, Murphy BJ, Ahr B, Robert-Hebmann V, Delauzun V, Nye KE, Devaux C, Biard-Piechaczyk M. Role of the intracellular domains of CXCR4 in SDF-1-mediated signaling. *Blood.* 2003;101:399–406. doi:10.1182/blood-2002-03-0978.
36. Zeng CM, Chen Z, Fu L. Frizzled receptors as potential therapeutic targets in human cancers. *Int J Mol Sci.* 2018;19(5):1543. doi:10.3390/ijms19051543. PMID: 29789460.
37. Marks JD, Hoogenboom HR, Bonnert HR, McCafferty TP, Griffiths J, Winter AD, By-Passing Immunization G. Human antibodies from V-gene libraries displayed on phage. *J Mol Bio.* 1991; Dec 5;222(3):581–97. doi:10.1016/0022-2836(91)90498-U.
38. Lee CM, Iorno N, Sierro F, Christ D. Selection of human antibody fragments by phage display. *Nat Protoc.* 2007;2:3001–08. doi:10.1038/nprot.2007.448. PMID: 18007636.